Excitation of the $3p^4(4s,3d,4p)$ Ar^+ states during Ar photoionization: Intensity, alignment, and orientation

Hugo W. van der Hart* and Chris H. Greene
JILA and Department of Physics, Campus Box 440, University of Colorado, Boulder, Colorado 80309-0440
(Received 23 January 2001; published 17 June 2002)

Ar photoionization is studied using the *R*-matrix formalism with emphasis on the simultaneous excitation of the residual Ar^+ ion. Cross sections have been obtained for excitation of the $3p^4(3d,4s,4p)$ states. A comparison with experiments having a resolution of 70 meV shows reasonable agreement for the position and shape of resonance structures. The relative magnitude of the resonances proves to be more elusive. The partial cross section for excitation of the $3p^4(^3P^e)4p\ ^2P^o_{3/2}$ and $^2D^o_{3/2}$ levels is treated in more detail. A comparison of *LS*-coupling calculations with high-resolution experimental results shows good agreement for both the excitation cross sections and the polarization of the fluorescence. We also predict the orientation for both levels. We demonstrate that the polarization of the fluorescence originating from the $^2D^o_{3/2}$ level can be employed to study spin-orbit effects in Ar photoionization.

DOI: 10.1103/PhysRevA.65.062509 PACS number(s): 32.10.Hq, 31.25.−v, 31.50.Df

I. INTRODUCTION

Developments in technology and in measurement techniques have considerably improved the capabilities of experiments employing high-frequency light sources. Due to improvements in the frequency resolution and intensities, it is now routinely possible to study photoionization processes with frequencies up to several tens of eV in fine detail. Simultaneously, new measurement techniques have enabled experimentalists to study the physical processes in high-energy photoionization with a resolution of a few meV. These advances have enabled experimentalists to provide a highly detailed picture of high-energy photoionization of various atoms. In particular, the noble-gas atoms have been investigated intensively, since, due to their large binding energies, the study of their photoionization properties requires light sources able to generate these high frequencies.

The determination of the physics generating the experimental results requires the development of sophisticated numerical approaches, which are able to describe the system under investigation in great detail. The experimental effort in describing the detailed atomic physics thus requires a continuous effort to push the boundaries of computational approaches. In order to explore these boundaries, we have decided to study the photoionization of Ar in more detail due to the wealth of past, present, and future experimental data, and due to the complexity of the photoionization spectra with simultaneous excitation of $3p^4n\ell$ states of the residual ion. This complexity has meant that to the best of our knowledge these rich photoionization spectra of Ar have only been subjected to a cursory inspection, and they thus constitute a prime testing ground for examining the capabilities and the limitations of present theoretical approaches.

Whereas since the first observation of doubly excited states of Ar created by photoionization [1], many experimental studies have been devoted to $3p$ and $3s$ photoemission from Ar [2–6], until recently, few experiments have investigated the probability to leave Ar^+ in a higher excited state after photoionization. For frequencies above 33.21 eV, photoionization with excitation of a $3s^23p^4n\ell$ doublet state in Ar^+ becomes energetically allowed. First studies have focused on the intensities of satellite lines at high frequencies [7], but since then investigations have studied the effects of doubly excited states on the photoionization behavior [8]. Advances in the combination of synchroton radiation sources with spectroscopic detection techniques have enabled experimentalists not only to observe the detached electron but also the radiation emitted from these residual Ar^+ states [6,9–11]. These experiments show a more detailed photoionization spectrum of Ar with excitation of the $3p^4(^3P^e)4p\ ^2P^o_{3/2}$ level [9] than obtained using electron spectroscopy, since the frequency of the emitted light is unique for the excited Ar^+ state. The polarization of the fluorescence has been observed as well [10,11], providing additional information on the angular momentum transferred to the ejected electron [12,13]. When the orientation of the residual Ar^+ states is measured as well, the cross sections of the partial photoionization channels can be extracted, thus providing quite a detailed insight into the photoionization properties.

Many theoretical approaches have been employed to predict and explain the experimental photoionization spectra. While the first studies obtained the nonresonant photoionization calculations [14–19], it took several years before theoretical calculations started to examine the influence of doubly excited states involving double excitations on photodetachment processes in Ar [20]. These relativistic Hartree-Fock configuration-interaction (CI) calculations were followed up by Wijesundera and Kelly [21] employing many-body perturbation theory. In both approaches, only a limited number of excited target states were included since the main focus was directed towards deriving the satellite intensities for the excitation of $3p^4(^1D^e)nd\ ^2S^e$ states of Ar^+ during photoionization. These photoionization calcula-

*Present address: Department of Applied Mathematics and Theoretical Physics, Queen's University Belfast, Belfast BT7 1NN, United Kingdom.

tions did, therefore, not yield the full, very rich, structure of Ar photoionization above 30 eV. For example, in Ref. [21] a structureless gap, which is not reproduced in experiment [6], is seen in between 32 and 35 eV.

In order to improve the description of the resonance structure for Ar in the photon energy range up to 38 eV, a region heavily investigated by current experimental work, we will present results for Ar photoionization, including the probability for leaving Ar in an excited state. To achieve this, we employ the *R*-matrix approach incorporating an extensive description of the Ar structure. As such, the study is comparable to the theoretical calculations presented in [22] for Ne. In a previous paper [23], we demonstrated the influence of the doubly excited states on the photoemission of $3s$ and $3p$ electrons, while we also determined the threshold excitation of the Ar^+ states. The experimental interest focusing on ionization with excitation to the $3p^4(^3P^e)4p\ ^2P^o$ state of Ar^+ [10] provides the impetus for a closer investigation of the photoexcitation of the $3s^23p^4n\ell$ Ar^+ states. In Sec. III A we will present theoretical estimates for low-resolution excitation spectra and compare them with experiment [8], while they will be analyzed in more detail in Sec. III B. In Sec. III C we present high-resolution spectra. The results for the polarization of the radiation emitted by the Ar^+ states will be presented in Sec. III D. These latter two studies will be related to the available experimental results [10,11]. Finally, to stimulate experimental interest, we show in Sec. III E our prediction for the orientation of the $3p^4(^3P^e)4p\ ^2P^o_{3/2}$ and $^2D^o_{3/2}$ levels.

In another study, we have illustrated that spin-orbit effects may have a significant influence on the excitation spectra for particular transitions [24]. These spin-orbit effects are obviously important for investigating the excitation of quartet states of Ar^+, and for the excitation of the $^2S^o$ state of Ar^+. For the other doublet states, however, the inclusion of spin-orbit effects to the photoexcitation spectrum can be considered to be of less importance. Although calculations in LS coupling will not provide full agreement with experiment, they will provide a first approximation. The spin-orbit interaction acts a perturbation to these results. By comparing experiment and theory, the present calculations can therefore assist in illustrating which effects in the photoionization are due to spin-orbit interactions. The polarization of the emitted radiation is more sensitive to spin-orbit interactions, and we will demonstrate some effects of spin-orbit coupling on the polarization in Sec. III D

In addition to the neglect of spin-orbit interactions, there is another limit to the present calculations. Above an energy of 38 eV, high-lying doubly excited states, which cannot be included in the calculations at present, become important. The accurate description of these doubly excited states requires additional target states and more continuum wave functions, resulting in a CI expansion which is too big for the computational resources at our disposal. We have therefore limited ourselves to a maximum photon energy of 38 eV.

II. THEORETICAL APPROACH

The present study has been performed using the multichannel quantum-defect *R*-matrix approach, as described by Aymar *et al.* [25]. In this approach, it is assumed that exchange effects involving the outer electron can be neglected at large distances. Hence, phase space can be separated into an inner and an outer region. In the inner region, the full electron dynamics is described, while in the outer region the outer electron is approximated as a free outgoing electron in the field of the residual ion. The photoionization properties can then be obtained by matching the inner region to the asymptotic solutions at the boundary. A major development in the application of this *R*-matrix theory has been the combination with another powerful approach in theoretical atomic physics, the multiconfiguration Hartree-Fock (MCHF) approach [26]. This development has been applied with good success to the study of aluminum [27] and neon [22]. Previous results for Ar using this approach [23,24] have demonstrated the capabilities of this approach in elucidating the resonance structure of Ar, and identify the appearance of effects due to the splitting of Ar^+ states due to spin-orbit couplings, and of effects due to spin-orbit induced mixing of Ar^+ levels with differing LS quantum numbers but identical J.

Accurate photoionization cross sections can only be obtained when both the initial and the final state of the atom are described precisely. The initial state is the ground state of Ar, while the final state is approximated as Ar^+ with a free electron. These final states can be degenerate with doubly excited states of Ar and hence a good description of both Ar and Ar^+ is required simultaneously. An important approximation for the description of Ar is that good states can be obtained by adding a single electron to well-described low-lying states of Ar^+. These Ar^+ states are described using MCHF orbitals. This is the preferred choice since we need a very good description using as few basis functions as possible.

The MCHF orbitals for the physical target states have been obtained in the following way. The $1s$, $2s$, $2p$, $3s$, and $3p$ orbitals have been obtained from a Hartree-Fock calculation for the average $1s^22s^22p^63s^23p^5$ configuration of Ar^+. The $3d$ orbital is obtained by a HF calculation for the average of $3p^43d$ in Ar^+, using the core orbitals obtained from the previous calculation. Similarly, a $4s$ orbital is obtained from a HF calculation for the average of $3p^44s$, and a $4p$ orbital is obtained from a HF calculation for the average of $3p^44p$.

In addition to physical target state orbitals, we also need correlation-type orbitals to improve the description of our target states. Orbitals $\overline{4d}$,$\overline{5s}$,$\overline{5p}$ are generated using the MCHF approach. The overline indicates that these orbitals are pseudoorbitals : they do not describe physical states. A configuration list containing single and double excitations from the $3s^23p^4(^1D^e)3d\ ^2S^e$ and the $3s3p^6\ ^2S^e$ states is generated using a basis set consisting of $3s$, $3p$, $3d$, and $\overline{4d}$. The $\overline{4d}$ orbital is now optimized on the $3s^23p^4(^2D^e)3d\ ^2S^e$ state using this list. The $\overline{5s}$ orbital is obtained by performing the same procedure for the $3s^23p^4(^1S^e)3d\ ^2D^e$ state using all single and double excitations in an active space containing $3s$, $3p$, $3d$, $4s$, and $\overline{5s}$. Finally, the $\overline{5p}$ orbital is obtained using a $3s$, $3p$, $4p$, and $\overline{5p}$ active space for generat-

TABLE I. Energies of Ar^+ states obtained in the *R*-matrix approach using MCHF orbitals and compared to the experimental results.

State	*R*-matrix (eV)	Experiment [28] (eV)
$3s^23p^5\,^2P^o$	0.000	0.0
$3s3p^6\,^2S^e$	12.937	13.421
$3s^23p^4(^3P^e)4s\,^2P^e$	17.452	17.123
$3s^23p^4(^3P^e)3d\,^2P^e$	18.336	17.962
$3s^23p^4(^1D^e)4s\,^2D^e$	18.696	18.384
$3s^23p^4(^3P^e)3d\,^2F^e$	19.109	18.488
$3s^23p^4(^3P^e)3d\,^2D^e$	19.124	18.643
$3s^23p^4(^1D^e)3d\,^2G^e$	19.607	19.059
$3s^23p^4(^3P^e)4p\,^2D^o$	20.098	19.654
$3s^23p^4(^3P^e)4p\,^2P^o$	20.211	19.786
$3s^23p^4(^1D^e)3d\,^2F^e$	20.924	20.201
$3s^23p^4(^1S^e)4s\,^2S^e$	20.904	20.685
$3s^23p^4(^1D^e)4p\,^2F^o$	21.532	21.077
$3s^23p^4(^1D^e)4p\,^2P^o$	21.831	21.318
$3s^23p^4(^1D^e)3d\,^2D^e$	22.205	21.329
$3s^23p^4(^1D^e)4p\,^2D^o$	22.002	21.437
$3s^23p^4(^1D^e)3d\,^2P^e$	23.079	21.582
$3s^23p^4(^1S^e)3d\,^2D^e$	22.993	22.224
$3s^23p^4(^1D^e)3d\,^2S^e$	23.573	22.766

ing all single and double excitations of the $3s^23p^4(^1S^e)4p\,^2P^o$ state.

After the generation of the orbitals, the next step in the calculations is the determination of good target states of Ar^+. The outermost shells $3s^N$ and $3p^M$ can be polarized easily, and in this step it is thus important to take configurations into account, which describe this polarization. This is especially important for obtaining accurate energies for Ar and Ar^+ simultaneously. For Ar, some core-polarization effects are accounted for, due to configurations such as $3s^23p^43dnd$, which interact with $3s^23p^6$. For Ar^+, the important core-excited states have to be included in a different approach.

Since the purpose of the study is the investigation of the excitation rates for the $3s^23p^4(3d,4s,4p)$ doublet states, all these target states obviously need to be included. Also the $3s^23p^4(\overline{4d},\overline{5s},\overline{5p})$ doublet states are included, as well as the $3s^23p^5\,^2P^o$ and the $3s3p^6\,^2S^e$ states. Core-polarization target states are now included by performing CI calculations for each one of the $3s^23p^5\,^2P^o$, $3s3p^6\,^2S^e$, and $3s^23p^4(3d,4s,4p)$ doublet states using all single and double excitations from these states within an active space of $3s$, $3p$, $3d$, $4s$, and $4p$. All configurations with a contribution of at least 0.1% are included in the expansion for the target states. On average, for each state, 99.4% of its composition is included in this way. Some configurations neglected for one state may be important for a different state, so the final inclusions will on average amount to more than 99.4%.

A CI calculation using this Ar^+ expansion gives the energies reported in Table I for states which can be excited by photoionization from the Ar ground state. A comparison with the experimental energies [28] shows that the disagreement in excitation energy is generally around 0.5 eV, but that for the highest $3s^23p^4(3d,4s,4p)$ states the differences increase up to 1.5 eV. These highest states lie close to the energy region where higher-lying $3p^4n\ell$ states are found and the neglect of these interactions will deteriorate the calculated energies. In fact, the $3s^23p^4(^1S^e)4p\,^2P^o$ state is immersed in these higher manifolds and no reliable theoretical prediction can be provided. Further, it should be noticed that the lowest excited states have got a too small excitation energy, indicating that also the Ar^+ ground state has not been obtained with a very high precision.

The Ar problem is now solved using the *R*-matrix approach. The inner-region boundary is set at a radius of 13 a.u. Basis states for Ar are generated by adding a complete set of single-electron basis functions, orthogonal to all the orbitals from the MCHF calculations, to the target states. The maximum angular momentum for the outer electrons is 3. Electrons with ℓ larger than 3 can be coupled to the $^2F^o$ and $^2G^e$ states mentioned in Table I, but the probability for emission of these high-ℓ electrons is expected to be negligible. The basis set contains 21 states for *s* and *p* electrons, 18 for *d* electrons and 16 for *f* electrons. The total basis expansion for the Ar photoionization problem then consists of 2350 states for the $^1S^e$ states and 5581 for the $^1P^o$ states. This number of states in the $^1P^o$ symmetry is chosen such that the computer program fully employs the maximum available computer memory. The energy of Ar is calculated to be 17.742 eV, compared to the experimental results of 15.819 eV. In order to obtain the proper transition frequencies, the Ar ground state and all Ar^+ states are shifted to the experimental values.

The Ar ground state is too strongly bound by about 2 eV in these calculations, which can be explained through core-polarization interactions. We include more basis functions, and hence more core excitations, for Ar than for Ar^+. When all possible excitations are included, the correct energy difference will be reproduced, but in other cases, the Ar binding energy is easily overestimated. The Ar^+ and the Ar basis size are inextricably linked to each other since consistency requires that a complete set of outer electron wave functions is added to all Ar^+ states for the Ar expansion. The only way, therefore, to improve on this overconvergence is by extending both basis sets. An increase in the basis set would however lead to a too large calculation to fit in the computer.

In order to get photoionization spectra starting at the proper transition frequency, both the Ar ground state and the Ar^+ target state energies have been shifted to the experimental values. For the Ar ground state, this poses no problems, since it is well isolated from other Ar states. For the Ar^+ target states, however, the usual approach [25] is to shift the Ar^+ thresholds after the determination of the *K* matrices. Thus, in the Ar calculation, the theoretical values for the Ar^+ energies would be used. This approach is easy to implement, but works better when the accuracy of the Ar^+ energies is quite good. The approach is less successful when the shifts are large. In the present case, it was found that this approach does not lead to fully stabilized results due to the number of Ar^+ states combined with their relatively large shifts to the experimental energies.

In order to improve the stability of the codes, the approach has therefore been modified. First, the Ar^+ Hamiltonian is diagonalized. We shift the Ar^+ energies to the proper energies by comparing the calculated energies with experiment. We then obtain a diagonal matrix containing the energy shifts. This matrix is transformed back to the original basis functions, providing energy shifts for each particular Ar^+ basis function. Since the Ar basis functions are represented as an Ar^+ state plus a continuum electron, we can then add these shifts to the Ar Hamiltonian. The only Ar configuration which is not uniquely defined as such is the $3s^2 3p^3 3d^3$ configuration. This configuration is not shifted. Diagonalization of the Ar Hamiltonian, which includes this correction to the Ar^+ eigenstates, leads to a much improved convergence for the Ar photoionization cross sections.

III. RESULTS

The calculations provide a substantial amount of data. For each target state, we obtain highly detailed information about the outgoing electron. Because of the wealth of data, only a limited amount can be presented. While we predict photoionization and excitation spectra for all available target states reachable with a photon energy of 38 eV, in the present report we limit our discussion to some of the channels which have been observed experimentally. First we will show a comparison between the present calculations and low-resolution experimental data [8]. Then we will compare our results with high-resolution spectra [10,11].

A. Low-resolution spectra of low-lying $3p^4 n\ell$ states

Low-resolution spectra of Ar photoionization with simultaneous excitation of the residual ion have been provided over a decade ago by Wills *et al.* [8]. The resolution of their detector was 70 meV, which is not sufficient to detect fine details of the Ar structure, but suffices to separate low-lying Rydberg states converging to the forest of Ar^+ final states. This resolution is, however, insufficient to separate all the Ar^+ states, so spectra were presented for, e.g., an excitation of the $3p^4(^3P^e)4p\,^2P^o$ and the $3p^4(^3P^e)4p\,^2D^o$ state combined. Not only can Ar^+ states overlap: for the $3p^4(^3P^e)3d\,^2F^o$ state, the different J levels overlap with different Ar^+ states. Since the different states are excited coherently, interference between the different photoionization channels may affect the probability to detach an electron. Also, one needs to know the probabilities to excite each of the states involved. Since we do not have this knowledge, an unambiguous comparison becomes difficult for states that overlap, and the present comparison is therefore limited to only those states for which no overlap is found.

The states for which overlap effects are negligible are the $3p^4(^3P^e)4s\,^2P^e$, $3p^4(^3P^e)3d\,^2P^e$, $3p^4(^1D^e)3d\,^2G^e$, $3p^4(^1D^e)3d\,^2F^e$, $3p^4(^1S^e)4s\,^2S^e$, and the $3p^4(^1D^e)4p\,^2F^o$ states. The same applies, in principle, also to the $3p^4(^1S^e)3d\,^2D^e$ and $3p^4(^1D^e)3d\,^2P^e$ states, but the excitation energy of these states is too high to expect a theoretical spectrum resembling experiment. In Figs. 1–3, spectra are presented for these states as a function of intensity and compared to the experimental results obtained by Wills *et al.* [8]. In order to obtain a fair comparison, the *R*-matrix results have been convolved with a Gaussian of 70 meV width, since the experimental resolution has a significant effect on the observed spectrum, e.g., by averaging out the individual states in a Rydberg series, as seen previously [23].

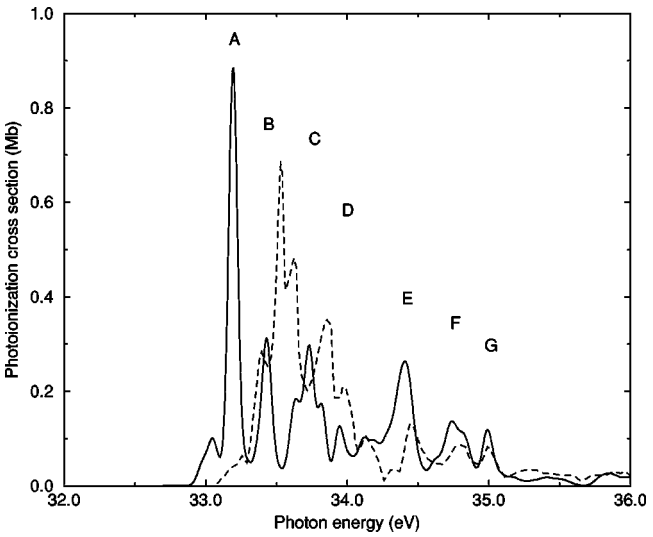

FIG. 1. Cross section for photoionization of Ar with excitation of the residual $3p^4(^3P^e)4s\,^2P^e$ state of Ar^+ in the photon energy range between 32 and 36 eV. The theoretical results (solid line) are compared to the experimental results of Wills *et al.* [8] (dotted line).

Another important point to bear in mind when comparing theory and experiment is the efficiency of the electron detec-

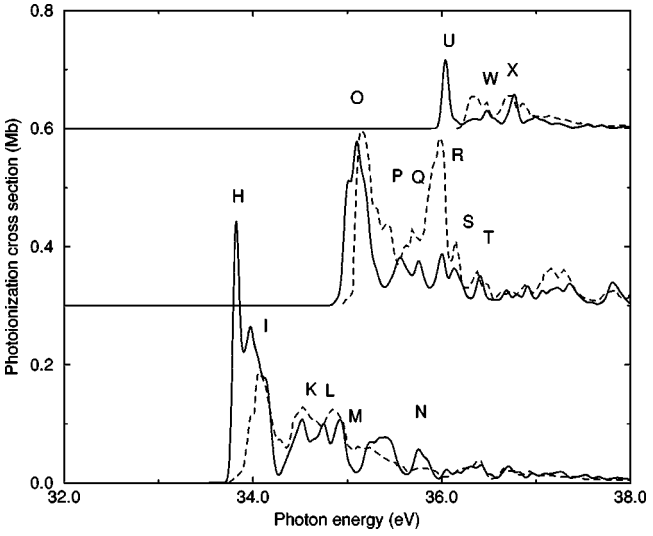

FIG. 2. Cross sections for photoionization of Ar with excitation of the $3p^4(^3P^e)3d\,^2P^e$, $3p^4(^1D^e)3d\,^2G^e$, and $3p^4(^1D^e)3d\,^2F^e$ states of Ar^+ in the photon energy region between 32 and 38 eV. The $3p^4(^1D^e)3d\,^2G^e$ excitation cross sections are shifted upward by 0.3 Mb, while the $3p^4(^1D^e)3d\,^2F^e$ excitation cross sections are shifted upward by 0.6 Mb. The theoretical results (solid line) are compared to the experimental results of Wills *et al.* [8] (dotted line).

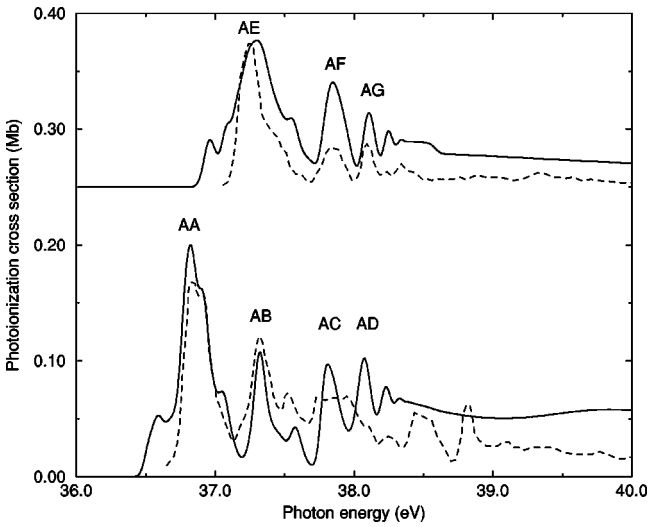

FIG. 3. Cross sections for photoionization of Ar with excitation of the residual $3p^4(^1S^e)4s\ ^2S^e$ state and the $3p^4(^1D^e)4p\ ^2F^o$ state of Ar^+ in the photon energy range between 36 and 40 eV. The photoexcitation cross sections for the $3p^4(^1D^e)4p\ ^2F^o$ state are shifted by 0.25 Mb. The theoretical results (solid line) are compared to the experimental results of Wills *et al.* [8] (dotted line). Above a photon energy of 38 eV, the approximations in the theoretical calculations are too severe for a proper comparison with experiment.

tors. It is very difficult to measure accurately emitted electron spectra at very small emission energies. Previously, we have compared theoretical threshold detachment cross sections [23] with experimental ones [30] and found quite a good agreement. This agreement therefore indicates the reliability of the calculations close to threshold, which cannot be established from the present comparisons.

Moderate agreement between theory and experiment is observed in the structure of the spectrum in Figs. 1–3. The line shapes of most resonances are in decent agreement with experiment, but the magnitude is not reproduced. The position of the resonances is in reasonable agreement with experiment, although some notable differences, up to 0.2 eV, are observed for several resonances. These differences may be due to the splitting of the Ar^+ states in the different J values and overconvergence of the Ar calculation. The splitting of the target states results in a splitting of the Ar states and a shift in the position of certain resonances.

The agreement of the experimental and theoretical photoionization spectrum shown in Fig. 1 is best at the higher photon energies. Resonances *E*, *F*, and *G* can easily be identified in the experimental spectrum. The identification of the other resonances is slightly more complicated, since it appears that the spectrum has been shifted by roughly 0.2 eV. Certain resonances may, however, have shifted more than 0.2 eV, and also the intensity of the resonances may be very different from the intensity observed experimentally. This latter problem is presumably strongest for resonances *A* and *B*, which seem to have their intensities reversed compared to experiment.

In Fig. 2, the agreement between theory and experiment is again best at the higher photon energies. In the bottom photoionization spectrum, for excitation of the $3p^4(^3P^e)3d\ ^2P^e$ state, the general agreement of the resonance spectrum is pretty good, apart from resonance *H*. Resonance *H* may be difficult to detect experimentally though due to the small electron ejection energy. The excitation of resonance *N* is overestimated by theory, and the appearance of window resonance *M* is also stronger than in experiment. In the middle photoionization spectrum, for excitation of the $3p^4(^1D^e)3d\ ^2G^e$ state, the main difference between experiment and theory appears to be the excitation strength of resonance *R*. If this resonance would be excited stronger, the theoretical and experimental results would agree very well. The agreement is worst for the top photoionization spectrum, for excitation of the $3p^4(^1D^e)3d\ ^2F^e$ state, in which only two resonances, W and X, appear in the theoretical spectrum, with little indication of the two other resonances, which are prominent in the experimental spectrum.

In Fig. 3, the agreement between theoretical and experimental resonances is very good again up to a photon energy of 38 eV for both photoionization spectra with excitation of the $3p^4(^1S^e)4s\ ^2S^e$ state (bottom) and the $3p^4(^1D^e)4p\ ^2F^o$ state (top). Above a photon energy of 38 eV, the limitations of the calculations become apparent. In these spectra, the assignment of the experimental resonances can be carried out reliably, although the relative excitation strengths are still not in very good agreement with experiment.

The overall agreement between the theoretical and experimental photoionization spectra is reasonably good. For some spectra, a very good description has been obtained, while for others the agreement is fairly poor. The problems with the assignment of experimental resonances can be solved for certain spectra.

B. Analysis of the theoretical photoionization spectra

An example of overconvergence of the Ar states is shown in Fig. 1 by resonances *A*, *B*, *C*, and *D*. Results for $3s$ photoemission have shown that the deviations in the quantum defect for the lowest $3p^4n\ell$ series can become quite large, in the order of 0.2 [23]. The difference in energy between the calculated and the experimental resonances is quite clear in Figs. 1–3. Nevertheless, the global structure of the calculated spectrum agrees nicely with the calculated one. In Table II we give positions and classifications of the resonances observed in the theoretical spectrum and their position in the experimental spectrum.

Although the classification of the resonances may give valuable clues to important interactions between Ar^+ states, we should take proper care in doing so. The classification of the resonances *A*–*G* in Fig. 1 seems to indicate that the interactions for photoionization with excitation of the $3p^4(^3P^e)4s$ state of Ar^+ are dominated by four closed channels. This is not entirely the case, however. The interactions are so complex for low-lying Rydberg states, that an unambiguous identification is impossible. The present identification follows from a close examination of the photoionization spectra, while for a definite assignment the true wave functions are required. Furthermore, because of the overlapping resonances, only the most dominant component has been as-

TABLE II. Identification of Ar^+ resonances in the partial photoionization spectra. OE stands for outer electron. All resonances appear as peaks except for resonances *J*, *K*, and *M* as explained in the text. Also the classification of resonances *B*, *C*, *D*, *E*, *F*, and *G* requires a careful discussion in the text.

Label	Energy (eV)	Ar^+ state	n^*	OE
A	33.19	$3s^2 3p^4(^1S^e)4s\ ^2S^e$	2.03	$4p$
B	33.43	$3s^2 3p^4(^1D^e)4s\ ^2D^e$	4.20	$6p$
C	33.73	$3s^2 3p^4(^3P^e)4p\ ^2P^o$	2.69	$5s$
D	33.95	$3s^2 3p^4(^1D^e)4s\ ^2D^e$	7.33	$9p$
E	34.41	$3s^2 3p^4(^3P^e)4p\ ^2D^o$	3.58	$4d$
F	34.74	$3s^2 3p^4(^3P^e)4p\ ^2P^o$	3.97	$5d$
G	34.99	$3s^2 3p^4(^3P^e)4p\ ^2P^o$	4.70	$7s$
H	33.82	$3s^2 3p^4(^1D^e)3d\ ^2F^e$	5.29	$5f$
I	33.97	$3s^2 3p^4(^1D^e)3d\ ^2P^e$	1.99	$4p$
K	34.61	$3s^2 3p^4(^3P^e)4p\ ^2P^o$	3.70	$6s$
L	34.82	$3s^2 3p^4(^3P^e)4p\ ^2D^o$	4.56	$5d$
M	35.06	$3s^2 3p^4(^1S^e)4s\ ^2S^e$	3.07	$5p$
N	35.75	$3s^2 3p^4(^1S^e)4s\ ^2S^e$	4.25	$6p$
O	35.10	$3s^2 3p^4(^1S^e)4s\ ^2S^e$	3.11	$5p$
P	35.56	$3s^2 3p^4(^1D^e)4p\ ^2F^o$	3.19	$4d$
Q	35.76	$3s^2 3p^4(^1S^e)4s\ ^2S^e$	4.28	$6p$
R	36.00	$3s^2 3p^4(^1S^e)4s\ ^2S^e$	5.20	$7p$
S	36.13	$3s^2 3p^4(^1D^e)4p\ ^2F^o$	4.21	$5d$
T	36.41	$3s^2 3p^4(^1D^e)4p\ ^2F^o$	5.29	$6d$
U	36.04	$3s^2 3p^4(^1D^e)4p\ ^2D^o$	3.34	$4d$
W	36.48	$3s^2 3p^4(^1D^e)4p\ ^2D^o$	4.19	$5d$
X	36.82	$3s^2 3p^4(^1D^e)4p\ ^2D^o$	5.29	$6d$
AA	36.82	$3s^2 3p^4(^1S^e)3d\ ^2D^e$	3.34	$5p$
AB	37.32	$3s^2 3p^4(^1S^e)3d\ ^2D^e$	4.34	$6p$
AC	37.81	$3s^2 3p^4(^1D^e)3d\ ^2S^e$	4.19	$6p$
AD	38.07	$3s^2 3p^4(^1D^e)3d\ ^2S^e$	5.14	$7p$
AE	37.30	$3s^2 3p^4(^1D^e)3d\ ^2S^e$	3.25	$5p$
AF	37.85	$3s^2 3p^4(^1D^e)3d\ ^2S^e$	4.30	$6p$
AG	38.11	$3s^2 3p^4(^1D^e)3d\ ^2S^e$	5.35	$7p$

signed. Other series could be important as well, but have a smaller contribution to a resonance. This is the case, for example, for resonances *F* and *G*, which are classified as belonging to the $3p^4(^3P^e)4p(^2P^o)n\ell$ series, while for both resonances there is an important contribution from the $3p^4(^3P^e)4p(^2D^o)n\ell$ series as well. The opposite is seen for resonance *E*.

In addition, Rydberg states belonging to different series may appear in the photoionization spectrum, wiping out any sign of regularity for states with principal quantum number $n<10$. An example of the effect of overlapping Rydberg series is observable for resonance *C*, which has two distinct shoulders. The identification of resonances *B* and *D* as the $6p$ and $9p$ members of the Rydberg series leading up to the $3s^2 3p^4(^1D^e)4s\ ^2D^e$ threshold allows the assignment of the shoulders of resonance *C* as the missing $7p$ and $8p$ members.

The photoionization spectrum in Fig. 1 cannot be understood fully by looking at this spectrum in isolation. For example, we need other spectra to find out that the main reason why resonances *C* and *D* are observed is not the direct excitation of these resonances. Instead the $3s^2 3p^4(^1D^e)3d(^2P^e)4p\ ^1P^o$ resonance is excited initially, which then redistributes its intensity, donating part of it to resonances *C* and *D*. These redistributions make a clear identification of the important resonances in the photoionization processes much more difficult. By examining the spectra at low resolution, we can obtain information about the global structure of the spectra, and see the low-Rydberg resonances, which are excited initially. With an improved resolution, the interaction between low-Rydberg and high-Rydberg states (in series converging to different thresholds) causes a redistribution of the excitation intensity to the high-Rydberg states, which may become distinguishable in high-resolution spectra. A complete analysis thus requires both high-resolution and low-resolution spectra for identifying the important interactions in doubly excited Ar.

One of the important experimental findings by Wills *et al.* [8] was that only resonances within 4 eV of the threshold were found to be excited. Figure 1 shows that the most prominent resonances are found within 1 eV of the Ar^+ threshold due to the sharp drop in overlap between the continuum electron and the doubly excited state [29]. For energies more than 4 eV above the threshold the entire excitation spectrum reduces to very small values for most Ar^+ states. Only for Ar^+ states, which contain contributions from either the $3s3p^6$ or the $3s^2 3p^5$ configurations, is a significant excitation expected at large energies above the threshold. The excitation of these Ar^+ states originates from direct photoemission of a $3s$ or $3p$ electron.

In Fig. 2, photoionization with excitation of the $3p^4(^3P^e)3d\ ^2P^e$ (bottom), $3p^4(^1D^e)3d\ ^2G^e$ (middle), and $3p^4(^1D^e)3d\ ^2F^e$ (top) states is presented together with the experimental results. Here, the agreement of the observed and theoretical resonance positions is much better than for the $3p^4(^3P^e)4s\ ^2P^e$ spectrum in Fig. 1, although the shape of the spectra is not as good. The theoretically observed resonances have been classified according to the labels given in Table II. Resonances close to the onset of the channel may be less apparent in the observed spectrum due to a decreased detection efficiency. For the photoionization with excitation spectra of the $3p^4(^3P^e)3d\ ^2P^e$ and the $3p^4(^1D^e)3d\ ^2F^e$ states, the resonances at the onset of opening the channel are assumed not to appear in the experimental spectra.

The spectra in Fig. 2 lend themselves for a more detailed summary of possible effects for overlapping Rydberg states. Destructive interference between overlapping resonances is observed for resonances *K* and *L*, which appear as window resonances on top of a broader structure, which can be identified visually (and checked by a more detailed examination) as a lower member of the series containing resonances *M* and *N*, the $3s^2 3p^4(^1S^e)4s(^2S^e)4p\ ^1P^o$ resonance. The interaction with this structure causes resonances *K* and *L* to autoionize towards a different Ar^+ state. However, in this other spectrum the $3s^2 3p^4(^1S^e)4s(^2S^e)4p\ ^1P^o$ structure may not be observable. Certain spectra may thus not explain how resonances *K* and *L* are excited. A full investigation of all

spectra at different resolutions is required to perform a complete analysis.

A very obvious example of how the interactions in Ar modify the regular behavior along a Rydberg series can also be seen in Fig. 2. Resonance *M* is a window resonance, but a resonance belonging to the same Rydberg series, resonance *O*, is observed as a clear peak in the theoretical spectrum for photoexcitation of the $3p^4(^1D^e)3d\,^2G^e$ threshold. This resonance shows the redistribution of the excitation probabilities in a clear fashion. The excitation of the resonance decreases the probability to leave Ar^+ in a particular excited state, and transfers it to a channel which leaves Ar^+ in a different excited state.

Further examples of overlapping resonances are resonances *H*, *U*, *W*, and *X*. Resonance *H* is the only strong resonance identified in Figs. 1–3, which has an *f* electron as the outer electron. It is unlikely that an *f* electron is excited directly from the $3s^23p^6$ state. Resonance *H* obtains its contribution through its interaction with the underlying $3s^23p^4(^1D^e)3d(^2P^e)4p\,^1P^o$ resonance. Resonances *U*, *W*, and *X* are given as sequential members of the same Rydberg series, but their intensities do not show any regularity.

Figure 3 illustrates how the same resonance appears in different ionization spectra. The observed resonances in Fig. 3 for photoionization with excitation of the $3p^4(^1S^e)4s\,^2S^e$ and $3p^4(^1D^e)4p\,^2F^o$ states of Ar^+ are indicated in Table II. The resonance structures can be identified unambiguously and excellent agreement is obtained for the position and line shapes of the resonances. The two spectra in Fig. 3 show a clear effect from the same Rydberg series near 38 eV, while at lower energies the structure differs substantially. In addition, although the energies of resonances *AE* and *AB* are nearly identical, their widths are quite different. These resonances indeed belong to different series. Resonances *AF* and *AC* as well as *AG* and *AD* differ by about 0.04 eV in energy, while they are associated with the same resonances. The energies are measured at the peak of the resonance and a different line shape of the resonance may consequently affect the energy.

The limitation of the present calculations to a maximum energy of 38 eV becomes apparent in Fig. 3. The sharp decrease of the excitation rate with increasing emitted electron energy is conspicuously absent for the $3p^4(^1S^e)4s\,^2S^e$ state, even though its contribution from $3s3p^6\,^2S^e$ is very small, 1% [7]. Also for the $3p^4(^1D^e)4ps\,^2F^o$ state, the photoexcitation cross section does not decrease rapidly. No physical closed Ar^+ channel is included in the outer region above an energy of 38.2 eV. The resonances at 38.5 and 38.8 eV can thus not be reproduced in the calculations.

C. High-resolution spectra of low-lying $3p^4n\ell$ states

Recently, high-precision measurements of the intensity and the polarization of radiation originating from the $3p^4(^3P^e)4p\,^2P^o_{3/2}$ level [10] and from various *J* levels of the $3p^4(^3P^e)4p\,^2P^o$ $3p^4(^3P^e)4p\,^2D^o$ and $3p^4(^1D^e)3d\,^2F^e$ states [11] of Ar^+ formed in Ar photoionization have been performed using polarized synchroton radiation [10]. This intensity is directly related to the photoionization cross section with excitation to this particular state. The accuracy of this technique is significantly higher than the accuracy with which electron energies can be evaluated, and the relative probability for excitation of the particular state can be determined to a much better degree.

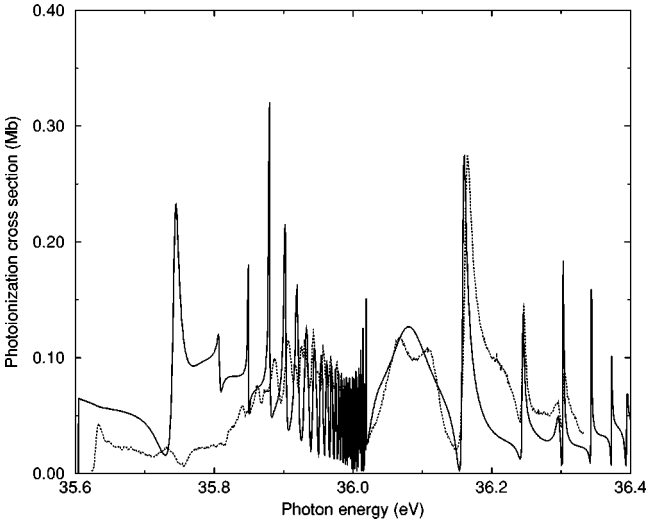

FIG. 4. Photoionization of Ar with excitation of the residual Ar^+ ion to the $3p^4(^3P^e)4p\,^2P^o$ state in the photon energy region between 35.6 and 36.4 eV. The theoretical results (solid line) are compared to the experimental ones (dotted line) are reported in [10].

The present calculation provides a theoretical description of the experimentally observed spectra for the spectra for photoionization with excitation of the $3p^4(^3P^e)4p\,^2P^o$ and $^2D^o$ states. The spectrum for photoexcitation of the $3p^4(^3P^e)4p\,^2P^o$ state in the photon energy range of 35.6 to 36.4 eV is shown in Fig. 4 and compared with the experimental results [10]. The agreement with the experimental data is very good, bearing in mind the limitations of the basis set employed in the present calculation. Several differences are noticeable, however, especially below 36 eV. Below 35.9 eV, the photoionization is significantly larger than observed experimentally, whereas the opposite is the case in between 35.9 and 36.0 eV. This difference is ascribed to a difference in position of several underlying resonances. In between 35.8 and 36.0 eV the background structure is mainly due to the Rydberg series leading up to the $^2S^e$ threshold. There are three additional resonances, which cause the large intensities for the peak at 35.72 eV and the one at 35.87 eV. The large intensity for the latter one is caused by the $3s^23p^4(^1D^e)4p(^2D^o)4d\,^1P^o$ resonance, while the former one is observed primarily due to its interaction with the $3s^23p^4(^1D^e)4p(^2P^o)4d\,^1P^o$ and $3s^23p^4(^1D^e)3d(^2D^e)5p\,^1P^o$ states. These states could be shifted to too low energies by roughly 0.05 to 0.1 eV, as indicated by the shifted position for the increase in the photoionization. The Rydberg series leading up to the $3p^4(^1D^e)3d\,^2F^e$ state of Ar^+ is therefore more pronounced at lower energies.

Above a photon energy of 36 eV, theory and experiment agree with alarming accuracy. The positions of the $8p$ state at 36.16 eV, $9p$ at 36.25 eV, and the higher members are determined with good accuracy. Even the shape of the $10p$

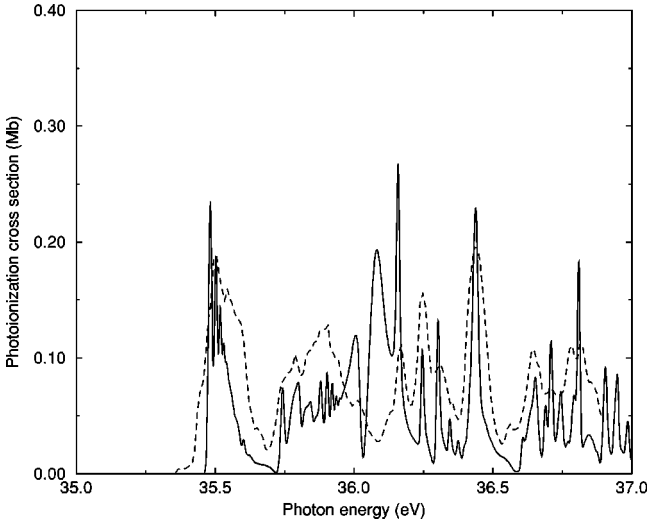

FIG. 5. Photoionization of Ar with excitation of the residual Ar^+ ion to the $3p^4(^3P^e)4p\ ^2D^o$ state. The theoretical results (solid line) are compared to the experimental results (dashed line) for the total photoemission with vertical polarization from the $J=5/2$ level of the $^2D^o$ state [11].

resonance at 36.30 eV, is described excellently. This resonance shows a deviation from a Fano profile, indicating the existence of an underlying resonance, the $3p^4(^1D^e)3d(^2D^e)4f\ ^1P^o$ resonance. The only difference between theory and experiment is that the splitting of the peak at 36.08 eV is not observed in the calculations.

Below a photon energy of 36 eV, there are some differences between theory and experiment in the position of the Rydberg series converging to the $3p^4(^1D^e)3d\ ^2F^e$ state. An explanation for this is the target state fine structure. The target states are split into the different J values. Due to the relativistic interactions, these target states have a different energy and consequently the Rydberg states are also shifted in energy. For the $3p^4(^1D^e)3d\ ^2F^e$ state, the splitting of the J levels is 25 meV [30], which satisfactorily explains the observed differences in the positions of the Rydberg states leading up to the $3p^4(^1D^e)3d\ ^2F^e$ state.

In the present calculations, we have neglected spin-orbit interactions, which are particularly important for the $3p^4(^3P^e)4p\ ^2P^o$ spectrum. The energy difference between the $3p^4(^3P^e)4p\ ^2P^o$ and the $^2D^o$ states is only 134 meV (see Table I), while their relativistic interaction is estimated to be 50 meV. The influence of spin-orbit coupling is discussed in more detail in [24] with some prominent examples. These examples demonstrate that it is important to study the photoionization cross sections with excitation of the $3p^4(^3P^e)4p\ ^2D^o$ state as well.

In Fig. 5, we show the photoionization spectrum in between 35.0 and 37.0 eV for the excitation of the $3p^4(^3P^e)4p\ ^2D^o$ state. These results are compared to experimental results which have been provided recently for the photoemission from the $J=3/2$ level [11]. Apart from the resonant behavior at 36.1 eV, which is not reproduced in experiment, very good agreement between theory and experiment is observed. The position of most resonances is reproduced in fine detail with maxima observed at the same position in both theory and experiment. The difference in intensity at 36.1 eV originates from the $3p^4(^1D^e)4p(^2P^o)6s\ ^1P^o$ resonance. This difference is presumably due to the fact that the theoretical spectrum is compared with the experimental spectrum for the $J=5/2$ level, whereas this resonance is observable mainly for the $J=3/2$ level [11].

Since the interference of the $3p^4(^3P^e)4p\ ^2D^o$ state with the $3p^4(^3P^e)4p\ ^2P^o$ state is of interest, a comparison of the two spectra could give some initial estimates about the effects of the interference. The overall intensity of the $^2D^o$ spectrum is very similar to the $^2P^o$ spectrum. The Rydberg series leading up to the $3p^4(^1D^e)3d\ ^2F^e$ state of Ar^+ has changed its behavior with a fairly small photoionization below 35.8 eV and increasing to a maximum at 36.0 eV. Above 36.0 eV, the changes are fairly small. The cross sections are larger by roughly 25% and the appearance of the resonance at 36.15 eV has changed. This points to different resonances having an influence on the photoionization spectra and a reduced effect of interferences.

As part of a previous investigation, we have obtained photoexcitation cross sections of the sublevels of the $3p^4(^3P^e)4p\ ^2D^o$ and the $3p^4(^3P^e)4p\ ^2P^o$ states after inclusion of an $LS \rightarrow jj$ frame transformation and spin-orbit interactions between the target states [24]. While the magnitudes of the resonances change, in particular, for the resonance at 36.1 eV for photoexcitation of the $^2D^o$ state, no fundamental difference in the spectra is observed. For these spectra, the main reason for the difference between experiment and theory is therefore the size of the basis set used in the calculations.

D. Alignment and polarization of radiation emitted by the $3p^4(^3P^e)4p\ ^2P^o_{3/2}$ and $^2D^o_{3/2}$ levels

The states of Ar^+ excited by the photoionization process are not stable, but decay to lower states through spontaneous emission of radiation. The different m values of each Ar^+ state are populated through photoionization and, in general, the different J levels will not be populated evenly. Consequently the fluorescence will be polarized. By monitoring this polarization for a particular transition in Ar^+, more detailed information can be obtained about the photoionization process, such as information about the probability for emission of an electron with a particular angular momentum.

Recent experimental results have been provided for the fluorescence polarization in Ar^+, monitoring the transition from the $3p^4(^3P^e)4p\ ^2P^o_{3/2}$ state to the $3p^4(^3P^e)4s\ ^2P^e_{1/2}$ state [10], as well as for the polarization of the fluorescence for the transition from the $3p^4(^3P^e)4p\ ^2P^o_{3/2}$ state to the $3p^4(^3P^e)4s\ ^2P^e_{3/2}$ state [11]. Here we will determine theoretically the polarization of the former radiative transition. Since this property depends on the coherence within states formed after emission of electrons with different angular momenta, this study provides a more stringent test for the theoretical calculations. In order to estimate roughly the effects of spin-order couplings, we will also present the fluorescence polarization for the transition from the $3p^4(^3P^e)4p\ ^2D^o_{3/2}$ state to the $3p^4(^3P^e)4s\ ^2P^e_{1/2}$ state.

The theory so far has been formulated in LS coupling. When the different J levels are monitored individually, this is no longer valid. This is the case experimentally, and theory thus needs to include the splitting of the LS-coupled states. The simplest approach is to employ a frame transformation to write the LS-coupled final state as a sum over jj-coupled final states by the following weighted 9-j symbol [31]:

$$T_{jj,LS}=[L,S,j_1,j_2]^{1/2}\begin{Bmatrix} l_1 & s_1 & j_1 \\ l_2 & s_2 & j_2 \\ L & S & J \end{Bmatrix} \tag{1}$$

with $[L]$ indicating $(2L+1)$. The index 1 refers to the final Ar^+ state, while the index 2 refers to the emitted electron. By multiplying the cross sections from Fig. 4 by the square of this transformation matrix element, the photoexcitation cross sections for the $J=1/2$ and $J=3/2$ levels of the $3p^4(^3P^e)4p\ ^2P^o$ state and the $J=3/2$ and $J=5/2$ levels of the $3p^4(^3P^e)4p\ ^2D^o$ state can be obtained. Here we are only interested in the $J=3/2$ levels.

A detailed description of the approach pursued to determine the polarization has been given by Greene and Zare [12]. The polarization is given by

$$P=\frac{3h^{(2)}(j_i,j_f)A_0^{col}(j_i)}{4+h^{(2)}(j_i,j_f)A_0^{col}(j_i)}, \tag{2}$$

with $h^{(2)}(j_i,j_f)$ a numerical factor depending on the initial and final angular momentum of the states involved in the radiative transition, j_i and j_f, respectively, given by

$$h^{(2)}(j_i,j_f)=\begin{cases} -j_i/(2j_i+3), & j_f=j_i+1 \\ 1, & j_f=j_i \\ -(j_i+1)/(2j_i-1), & j_f=j_i-1. \end{cases} \tag{3}$$

The alignment is obtained as outlined previously [24].

In Fig. 6, the polarization of the radiation for the transitions between the $3p^4(^3P^e)4p\ ^2P^o_{3/2}$ and the $3p^4(^3P^e)4s\ ^2P^e_{1/2}$ levels and between the $3p^4(^3P^e)4p\ ^2D^o_{3/2}$ and the $3p^4(^3P^e)4s\ ^2P^e_{1/2}$ levels are given after the former state is excited through photoionization from the ground state of Ar. For the latter polarization, a constant value of $-7/11$ is expected since only d electrons can be coupled to this target state to obtain a $^1P^o_1$ final state. The ionization channels with $d_{3/2}$ and $d_{5/2}$ outgoing electrons are linked by two weighted 9-j symbols and have a constant phase relationship. No interference can therefore occur and a value of $-7/11$ can be derived directly.

For the polarization of the radiation emitted from the $3p^4(^3P^e)4p\ ^2P^o_{3/2}\rightarrow 3p^4(^3P^e)4s\ ^2P^e_{1/2}$ transition, the agreement between theory and experiment is very good qualitatively, although generally the magnitude of the polarization is larger than observed experimentally by about 0.1. The main structure effects are described well. The shape of the polarization spectrum between 35.7 eV and 36.0 eV originating from the Rydberg series converging to the $3p^4(^1D^e)3d\ ^2F^e$ state is in good agreement, although several

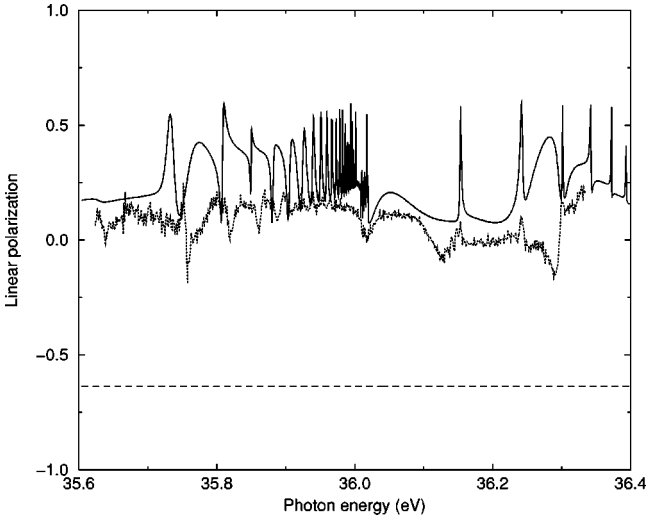

FIG. 6. Polarization of the radiation emitted when the $J=3/2$ level of the excited state of Ar^+ decays radiatively to the $3p^4(^3P^e)4s\ ^2P^e_{1/2}$ level. The solid line indicates the polarization for the $3p^4(^3P^e)4p\ ^2P^o$ state, while the dashed line indicates the polarization for the $3p^4(^3P^e)4p\ ^2D^o$ state. The experimental results (dotted line) are obtained from [10].

resonance features are slightly shifted from experiment. This provides an additional indication for the previous assertion that underlying theoretical resonances may disagree from their experimental position by roughly 0.05 to 0.1 eV. The dip at 36.0 eV is reproduced well. The main disagreements are observed at 36.15 eV and 36.30 eV, where the dips in the polarization are not reproduced theoretically, while the magnitude of the polarization seems to be overestimated at the resonances. The absence of the dip at 36.3 eV can be explained by an underlying resonance whose position is off by roughly 0.05 eV. Generally, the polarization spectrum shows that the structure effects originating from the $s_{1/2}$ photoemission channel interfering with the $d_{3/2}$ and $d_{5/2}$ photoemission channels are described reasonably well and, hence, that a satisfactory description of the individual photoemission channels has been obtained.

Since the structure is determined by the interference between s and d channels, an admixture of photoionization with excitation of the isoconfigurational $^2D^o$ state into the $^2P^o$ state may alter the observed polarization. This admixture will cause interference between the contribution from the emission of d electrons, while for s electrons the $^1P^o$ contribution is diminuished due to the admixture of the $^1D^o$ channel. The responsible interactions are relativistic in origin, the main one being spin-orbit interaction. Mentzel *et al.* [11] observed that the polarization of the Ar^+ fluorescence emitted by the $^2D^o_{3/2}$ state towards the $3p^4(^3P^e)4s\ ^2P_{3/2}$ state shows a significant amount of structure. Since in LS coupling, only d electrons can be emitted, leading to a constant polarization, the existence of this structure indicates the influence of relativistic interactions. Another recent demonstration of the influence of spin-orbit interactions is the ratio between the amplitude of $d_{5/2}$ and $d_{3/2}$ outgoing electrons during photoionization of Ar with simultaneous excitation of the $3p^4(^3P)4p\ ^2P^o_{3/2}$ level [32]. In LS coupling a constant

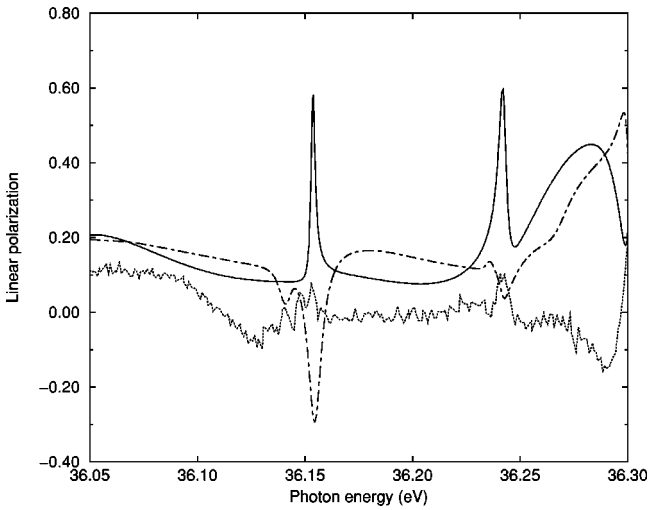

FIG. 7. Polarization of the radiation emitted when the $J=3/2$ level of the $3p^4(^3P^e)4p\ ^2P^o$ state of Ar^+ decays radiatively to the $3p^4(^3P^e)4s\ ^2P^e_{1/2}$ level. The solid line indicates the polarization obtained in LS coupling, while the dashed line indicates the polarization obtained after inclusion of a $LS \rightarrow jj$ frame tranformation and spin-orbit coupling of the target states. The experimental results (dotted line) are obtained from [10].

ratio of 3/2 is expected. Experimentally, however, the ratio is significantly larger than this value for photon energies between 35.8 and 36.1 eV.

The difference between experiment and theory can, however, not fully be ascribed to the neglect of spin-orbit interactions. We examine radiation from the $3p^4(^3P^e)4p\ ^2P^o_{3/2} \rightarrow 3p^4(^3P^e)4s\ ^2P^e_{1/2}$ transition after photoionization. The effects of spin-orbit coupling on the photoionization with excitation cross sections are relatively minor: apart from a statistical factor, the differences are primarily a change in the excitation strengths of the resonances. The effects of the spin-orbit coupling on the polarization of the radiation can, however, be quite significant. Figure 7 compares the polarization of the radiation from the $3p^4(^3P^e)4p\ ^2P^o_{3/2} \rightarrow 3p^4(^3P^e)4s\ ^2P^e_{1/2}$ transition in LS coupling, with the polarization obtained after an $LS \rightarrow jj$ frame transformation and, most importantly, the inclusion of spin-orbit interactions between the target states [24]. The given interval shows in detail a part of the spectrum where the effects of spin-orbit coupling are most dramatic. The peak at 36.15 eV changes sign, but still represents a change in magnitude of 0.4. The peak at 36.25 eV drops in magnitude from 0.4 to 0.1. In addition, the overall polarization is still larger than seen experimentally. The comparison therefore demonstrates that, although important, the inclusion of spin-orbit effects is not sufficient to explain the differences between the experiment and the present calculations in LS coupling in detail.

E. Orientation of radiation emitted by the $3p^4(^3P^e)4p\ ^2P^o_{3/2}$ and $^2D^o_{3/2}$ levels

The same information that is needed to extract the alignment and the photoexcitation cross section can also be employed to determine the orientation of the Ar^+ levels excited after photoionization employing circular polarized light. The orientation of a particular level with total angular momentum j_i is given by an equation similar to that employed for the alignment [12,24]:

$$O_0^{col}(j_i) = \frac{\sum_{j_t=j_i-1}^{j_i+1} |S(j_i,j_t)|^2 O_0^{col}(j_i,j_t)}{\sum_{j_t=j_i-1}^{j_i+1} |S(j_i,j_t)|^2}. \tag{4}$$

In this equation $|S(j_i,j_t)|^2$ again gives the cross section for excitation of a particular target state with angular momentum j_i and emission of an electron with angular momentum j_t. The limits on the sum follow from the $J=1$ symmetry of the state reached after absorption of a single photon from the $J=0$ ground state of argon. The factor $O_0^{col}(j_i,j_t)$ is the universal alignment function, following [13]

$$O_0^{col}(j_i,j_t) = \begin{cases} -\dfrac{qj_i/2}{\sqrt{j_i(j_i+1)}}, & j_t = j_i+1 \\ \dfrac{q/2}{\sqrt{j_i(j_i+1)}}, & j_t = j_i \\ \dfrac{q(j_i+1)/2}{\sqrt{j_i(j_i+1)}}, & j_t = j_i-1. \end{cases} \tag{5}$$

In this equation q indicates the helicity of the incident photon: linearly polarized light has $q=0$, left-circularly polarized light has $q=1$, and right-circularly polarized light has $q=-1$.

The orientation of the Ar^+ levels left after photoionization is related to the circular polarization P_C of the fluorescence emitted by these levels. The relationship is given by

$$P_C = -\frac{1}{2}\frac{3h^{(1)}(j_i,j_f)O_0^{col}(j_i)(P-3)\cos\theta}{P\cos^2\theta - 1}, \tag{6}$$

where P represents the linear polarization for the same transition and θ indicates the angle between the propagation directions of the incoming photon and the detected fluorescence photon. $h^{(1)}(j_i,j_f)$ is a geometrical factor given by [13]

$$h^{(1)}(j_i,j_f) = \begin{cases} -j_i/\sqrt{j_i(j_i+1)}, & j_f = j_i+1 \\ 1/\sqrt{j_i(j_i+1)}, & j_f = j_i \\ (j_i+1)/\sqrt{j_i(j_i+1)}, & j_f = j_i-1. \end{cases} \tag{7}$$

It should be emphasized that the definitions of the orientation O_0^{col} and the geometrical factor $h^{(1)}(j_i,j_f)$ differ by a factor $\sqrt{j_i(j_i+1)}$ and $1/\sqrt{j_i(j_i+1)}$ from those presented by Fano and Macek [33].

In Fig. 8, we show the polarization of the $3p^4(^3P^e)4p\ ^2P^o_{3/2}$ and $^2D^o_{3/2}$ levels after excitation during photoionization by a left-circular polarized photon ($q=1$). It can be seen that the shape of the spectra is very similar to the

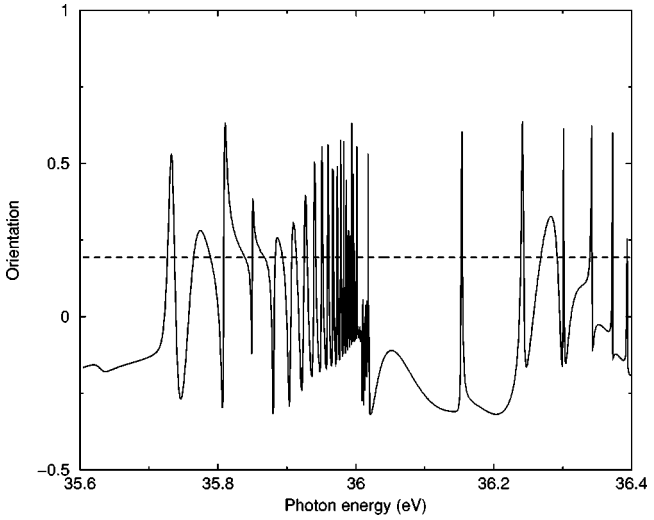

FIG. 8. Orientation of the $3p^4(^3P^e)4p\ ^2P^o_{3/2}$ (solid line) and $^2D^o_{3/2}$ levels (dashed line) of Ar^+ after excitation during photoionization of ground-state Ar by a left-circularly polarized photon.

alignment spectra, shown in Fig. 6. For the orientation of the $3p^4(^3P^e)4p\ ^2D^o_{3/2}$ level, this is obvious. In LS coupling the outgoing electron must be a d electron. This leads to a fixed relation between the channel probabilities and thus to a constant orientation. For the orientation of the $3p^4(^3P^e)4p\ ^2P^o_{3/2}$ level, the explanation is different. In LS coupling, both s and d electrons can be emitted. The normalized contributions from these two channels are added incoherently to form both the alignment and the orientation. The total alignment (or orientation), therefore varies between the alignment given if only d electrons contribute and the alignment given if only s electrons contribute. In fact, both the alignment and the orientation depend linearly on the contributions from both channels to the total photoionization. Thus, although the magnitude of the alignment and the orientation will differ, the shape of the spectrum will be similar.

The similarity of the orientation and alignment spectra under the assumption of LS can be exploited experimentally to demonstrate influences from spin-orbit coupling. Any difference in the shape of the orientation spectra for the $3p^4(^3P^e)4p\ ^2P^o_{3/2}$ and $3p^4(^3P^e)4p\ ^2D^o_{3/2}$ compared to the alignment spectra cannot be explained in LS coupling, and is hence most likely to be caused by spin-orbit coupling.

Furthermore, with knowledge about the total ionization cross section, the alignment, and the orientation, the contributions from the three partial channels can be obtained. (The three partial channels for leaving a state with angular momentum j_i have an angular momentum for the outgoing electron j_t of j_i-1, j_i, j_i+1.) Each of the three measurements gives a particular linear combination of the three partial channels, so that three measurements give a solvable linear system of three equations with three unknowns. Deviations from LS coupling can now become easier to spot by comparing outgoing electron channels with identical orbital angular momentum but different j.

IV. LIMITATION OF THE PRESENT CALCULATIONS

The study of Ar photoionization with the excitation of high-lying excited states in the residual ion constitutes a severe challenge for the theorist. Subtle effects in the photoionization are being determined, while the computational resources, though substantial, are too small to take all physical processes, required for a very accurate determination of the photoionization cross sections, into account. This results in severe approximations, which may influence the results considerably. Many Ar^+ configurations have been left out of the calculation, since they contributed less than 0.1% to the CI wave functions of the Ar^+ target states. All $Ar^+3p^4n\ell$ states with $n>6$ ($n>5$ for ℓ equal to 2 or 3, $n\geqslant 5$ for $\ell\geqslant 4$) have been neglected, which is especially for the higher states considered here a severe approximation. All states with an electron with $\ell\geqslant 4$ have been excluded.

Several Ar states are bound stronger to their threshold in the calculations than in experiment. As explained in the description of the calculations, the reason for this is the much larger basis for Ar than for Ar^+, which causes an overconvergence for Ar. This problem can be solved by increasing the size of the basis set, but that would make the calculations too big for the computers. This problem is the first reason for the differences between theory and experiment.

A different problem is the optimization of several orbitals. The $3d$, $4s$, and $4p$ orbitals are optimized on the average of the $3p^4n\ell$ configurations of Ar^+. However, for several states, these orbitals are not the most appropriate ones. This has been counteracted by including the pseudoorbitals, but it is unclear up to what extent this is an accurate description for all Ar^+ states.

A third major approximation is the use of LS coupling. Frame transformation techniques can be applied [24], but this remains a perturbative approach applicable only where spin-orbit interactions mainly influence the splitting of the target states. Since spin-orbit interactions mix some Ar^+ states strongly, these interactions may need a more detailed treatment. The full inclusion of relativistic interactions will again increase the computational resources required beyond the present limits.

Despite these approximations and difficulties, generally a spectrum is generated that reproduces the most important features observed in experiment. The energies of the states can be off the experimental results by up to 0.5 eV, but the shape of each individual resonance is in good agreement with experiment. The main reason for the disagreement between theory and experiment is therefore assigned to the incorrect positioning of several resonances in the calculations.

V. CONCLUSIONS

In the present study, we have obtained photoionization cross sections for Ar including the probability for exciting the residual Ar^+ ion to the lowest $3s^23p^4n\ell$ states. The eigenchannel R-matrix approach has been employed using MCHF wave functions to describe the states of Ar^+ as accurately as possible using a quite limited basis set. In view of this limitation, good energies are obtained for the lowest 20 states of Ar^+ and for the ground state of Ar. By adjusting the Ar Hamiltonian to take shifts of the Ar^+ states into account, more stable photoionization results are obtained.

In the photon energy range from 30 to 38 eV, 17 doublet $3s^23p^4n\ell$ states of Ar^+ can be excited. We have provided excitation rates in photoionization processes for these states

including a full *ab initio* calculation of the $^1P^o$ structure of Ar in this photon energy range. The atomic structure has a huge influence on the photoionization with excitation cross sections, with resonances considerably enhancing the excitation rates within 2 eV of the opening of the photoionization channel. For larger energies, the influence of resonances quickly decreases. The structure observed in experiment is reproduced, although the position of individual resonances may be off by 0.2 eV from the experimental positions. Line shapes are reproduced reasonably well, indicating that the interaction between the channels is described nicely. The main difficulty in the calculations is to accurately calculate the excitation strengths of the resonances. This difficulty is enhanced, in particular, by incorrect positions of the low-lying members of the Rydberg series.

By identifying observed resonances in the experimental spectrum, it is possible to obtain insight into the various interactions between the different photoionization channels. Since the spectrum contains many interacting resonances, knowledge of the experimental resolution is essential for a proper identification of the observed resonances. Detailed comparisons have been carried out for excitation of the $3p^4(^3P^e)4p\,^2P^o$ and $^2D^o$ states. Theory is able to explain the structures seen in these high-resolution experiments, while also the position of most resonances is reproduced.

The present *R*-matrix calculations have provided polarization spectra for fluorescent transitions following Ar photoionization leaving Ar^+ in the $3p^4(^3P^e)4p\,^2P^o_{3/2}$ or $^2D^o_{3/2}$ levels. It is shown that *LS* coupling leads to quite a reasonable agreement between theory and experiment for the $3p^4(^3P^e)4p\,^2P^o_{3/2}$ level. However, a substantial overall difference in the polarization between experiment and theory can be observed, which is ascribed to the size of the basis used as well as a neglect of spin-orbit couplings. This neglect becomes more prominent in the polarization spectrum of fluorescence from the $3p^4(^3P^e)4p\,^2D^o_{3/2}$ level, for which the presence of resonance structures in experiment [11] indicates the presence of spin-orbit effects. Due to the effects of a restricted basis set, the most reliable determination of the importance of spin-orbit coupling is through the study of features that are absent in *LS* coupling.

The present approach shows that reasonable results can be obtained for photoionization with excitation of fairly high-lying states of the residual system. Nevertheless several limitations of the present implementation have been identified. Improved results can be obtained by introducing frame transformation techniques to describe spin-orbit effects [24]. More importantly, the position of various resonances is described only within 0.2 eV, which has to be improved in order to obtain better agreement with experiment. Since this difference is ascribed to a different level of inclusion of core-polarization contributions for the Ar and the Ar^+ configurations, many more basis states need to be included in the calculations, requiring larger computers. When we bear in mind these difficulties, the present approach demonstrates that in the last decade, computational power has advanced to enable a sufficiently accurate description of the Ar structure in photoionization processes, to meaningfully compare experiment and theory up to a photon energy of 38 eV.

ACKNOWLEDGMENTS

The authors would like to thank F. Robicheaux for valuable discussions and O. Yenen and G. Mentzel for supplying numerical data of their results. This work was supported by the Division of Chemical Sciences, Office of Basic Energy Sciences, Office of Energy Research, U.S. Department of Energy. This research used resources of the National Energy Research Scientific Computing Center, also supported by the U.S. Department of Energy.

[1] R.P. Madden and K. Codling, Phys. Rev. Lett. **10**, 516 (1963).
[2] J.A.R. Samson, Adv. At. Mol. Phys. **2**, 177 (1966).
[3] J.B. West and G.V. Marr, Proc. R. Soc. London, Ser. A **349**, 397 (1976).
[4] J.A.R. Samson and J.L. Gardner, Phys. Rev. Lett. **33**, 671 (1974).
[5] R.G. Houlgate, J.B. West, K. Codling, and G.V. Marr, J. Electron Spectrosc. Relat. Phenom. **9**, 205 (1976)
[6] B. Möbus, B. Magel, K.-H. Schartner, B. Langer, U. Becker, M. Wildberger, and H. Schmoranzer, Phys. Rev. A **47**, 3888 (1993).
[7] H. Kossmann, B. Krässig, V. Schmidt, and J.E. Hansen, Phys. Rev. Lett. **58**, 1620 (1987).
[8] A.A. Wills, A.A. Cafolla, F.J. Currell, J. Comer, A. Svenson, and M.A. MacDonald, J. Phys. B **22**, 3217 (1989)
[9] J.A.R. Samson, E.M. Lee, and Y. Chung, J. Electron Spectrosc. Relat. Phenom. **66**, 75 (1993).
[10] O. Yenen, K.W. McLaughlin, and D.H. Jaecks, Phys. Rev. Lett. **79**, 5222 (1997).
[11] G. Mentzel, O. Wilhelmi, B. Magel, K.-H. Schartner, F. Vollweier, S. Lauer, and H. Schmoranzer, J. Phys. B **31**, 227 (1998).
[12] C.H. Greene and R.N. Zare, Phys. Rev. A **25**, 2031 (1982).
[13] C.H. Greene and R.N. Zare, Annu. Rev. Phys. Chem. **33**, 119 (1982).
[14] E.J. McGuire, Phys. Rev. **175**, 20 (1968).
[15] A.F. Starace, Phys. Rev. A **2**, 118 (1970).
[16] M.Ya. Amusia, N.A. Cherepkov, and L.V. Chernysheva, Zh. Eksp. Teor. Fiz. **60**, 160 (1971) [Sov. Phys. JETP **33**, 90 (1971)].
[17] C.D. Lin, Phys. Rev. A **9**, 171 (1974).
[18] P.G. Burke and K.T. Taylor, J. Phys. B **8**, 2620 (1975).
[19] T.N. Chang, Phys. Rev. A **18**, 1448 (1978).
[20] W.T. Silfvast, D.Y. Al-Salameh, and O.R. Wood II, Phys. Rev. A **34**, 5164 (1986).
[21] W. Wijesundera and H.P. Kelly, Phys. Rev. A **39**, 634 (1989).
[22] K. Schulz, M. Domke, R. Püttner, A. Gutiérrez, G. Kaindl, G. Miecznik, and C.H. Greene, Phys. Rev. A **54**, 3095 (1996).
[23] H.W. van der Hart and C.H. Greene, Phys. Rev. A **58**, 2097 (1998).

[24] H.W. van der Hart and C.H. Greene, J. Phys. B **32**, 4029 (1999).
[25] M. Aymar, C.H. Greene, and E. Luc-Koenig, Rev. Mod. Phys. **68**, 1015 (1996).
[26] C. Froese Fischer, T. Brage, and A. Jönsson, *Computational Atomic Structure: An MCHF Approach* (IOP, Bristol, 1997).
[27] G. Miecznik, C.H. Greene, and F. Robicheaux, Phys. Rev. A **51**, 513 (1995).
[28] L. Minnhagen, Ark. Fys. **25**, 203 (1963).
[29] J.E. Hansen, J. de Physique C **1**, 603 (1989).
[30] S. Cvejanovic, G.W. Bagley, and T.J. Reddish, J. Phys. B **27**, 5661 (1994)
[31] R.D. Cowan, *Theory of Atomic Structure and Spectra* (University of California Press, Berkeley, 1981).
[32] K.W. McLaughlin, O. Yenen, D.H. Jaecks, T.J. Gay, M.M. Sant'anna, D. Calabrese, and B. Thaden-Jordan, Phys. Rev. Lett. **88**, 123003 (2002).
[33] U. Fano and J.H. Macek, Rev. Mod. Phys. **45**, 553 (1973).